Chinese Physics Letters

PAPER

Head-on Collision of Solitary Waves Described by the Toda Lattice Model in Granular Chain

To cite this article: Qianqian Wu *et al* 2020 *Chinese Phys. Lett.* **37** 074501

CHIN. PHYS. LETT. Vol. 37, No. 7 (2020) 074501

Head-on Collision of Solitary Waves Described by the Toda Lattice Model in Granular Chain

Qianqian Wu(武倩倩)[1], Xingyi Liu(刘行易)[1], Tengfei Jiao(矫滕菲)[1], Surajit Sen[2*], and Decai Huang(黄德财)[1*]

[1] *Department of Applied Physics, Nanjing University of Science and Technology, Nanjing 210094, China*
[2] *Department of Physics, State University of New York, Buffalo 14260-1500, USA*

(Received 18 March 2020; accepted 5 May 2020; published online 21 June 2020)

We study the head-on collision of two solitary waves in a precompressed granular chain using the discrete element method. Our study takes the Toda chain solution as the initial condition for the simulations. The simulation covers the dynamical evolution of the collision process from the start of the incident wave to the end of the collision. The interaction has a central collision region of about five-grain width in which two solitary waves merge completely and share only one peak. Four stages, i.e., the pre-in-phase traveling stage, lag-phase collision state, lead-phase collision state, and post-in-phase traveling stage, are identified to describe the complex collision processes. Our results may be helpful for explaining the existence of long-lived solitary waves seen in the simulations by Takato and Sen [*Europhys. Lett.* 100 (2012) 24003].

PACS: 45.70.−n, 47.35.Fg, 05.45.−a, 04.60.Nc DOI: 10.1088/0256-307X/37/7/074501

Major milestones in nonlinear dynamics include the notion of the solitary wave (SW) that was first observed by Scott Russell in 1834 and the introduction of the Korteweg deVries (KdV) equation in 1895.[1] The SW has been extensively observed in nature, such as in a solid lattice,[2] biological molecules[3] and optical systems.[4] In 1983, Nesterenko found that SWs can be generated in granular chains (GCs) when an impulse is initiated at one end of the GC.[5] Both theoretical and experimental results established that the SW generated propagates with a width of about 11 grains when measured at sufficiently high accuracies and the width is independent of propagation velocity.[6–8] Recent works suggest that the study of impulse propagation in the GC has practical applications such as in nanoprinters,[9] acoustic diodes,[10,11] and sound dampers.[12,13]

The unique propagation characteristics of SWs in GCs stems from the strongly nonlinear interactions.[14,15] For a highly precompressed GC (PGC), Herbold and Nesterenko[16] employed the long wavelength approximation and constructed an analytical solution in the weakly nonlinear limit of the PGC system. The SW solution they obtained was that of a KdV system.[5,17] The KdV solution has been employed to describe incident waves to study collision properties of head-on propagating solitary waves (HSWs) in GCs. In the case of KdV solution, the incident SWs retain their original shapes and amplitudes after the collision.[18] No phase shift is found in both analytical and simulated results. However, when instead the analytic SW solution of the Toda lattice (TL) is used as an initial condition in the equations of motion for the Hertz system, one finds some oscillatory wave formation post collision of the SWs in the simulations. This result is different from the results obtained when using the same solution in the TL itself.[19] The trailing waves resulted from the collision of SWs are likely related to the critical PGC recently probed in Ref. [20]. To further explore the dynamical collision, we revisit the problem of the collision of HSWs described using the solution of the TL as the initial condition in a PGC.

We consider an alignment of N identical elastic grains with same mass m and radius R arranged between two fixed walls. At the outset the GC is precompressed by adjusting the distance between the two walls. The discrete element method is adopted to describe the motion of each grain. The Hertz interaction force without dissipation between two adjacent grains is only calculated in the normal direction. The grain is spherical and the Hertz model is used,[21,22]

$$F_i^{\rm H} = k_n[\delta_0 + (u_{i-1} - u_i)]_+^{3/2}, \tag{1}$$

where $[+] = \max[0, \delta_0 + (u_{i-1} - u_i)]$ is omitted henceforth, i is the index of the grain, δ_0 is the precompression between the adjacent particles, u_i denotes the displacement of the ith grain from its equilibrium position, k_n is the elastic coefficient calculated by $k_n = \frac{2E}{3(1-\nu^2)}(R/2)^{1/2}$, with E being the Young modulus and ν the Poisson ratio. The interaction force between the grain and the wall is treated as grain-grain interaction except that the wall has an infinite mass.

In a simulation time step, the position and velocity of each grain is updated by integrating Newton's second law of motion. According to Eq. (1), grain i will move according to the following equation,

$$mu_i'' = k_n[\delta_0 + (u_{i-1} - u_i)]^{3/2} - k_n[\delta_0 + (u_i - u_{i+1})]^{3/2}, \tag{2}$$

Supported by the National Natural Science Foundation of China (Grant No. 11574153).
*Corresponding author. Email: sen@buffalo.edu; hdc@njust.edu.cn

where the prime $'$ is the derivation with respect to t. For comparison of numerical simulation and analytical solution, m and k_n are set to unity. The simulation step time is set to $dt = 10^{-4}$. Taylor expansion is used and Eq. (2) becomes

$$\ddot{x}_i = (x_{i-1} - 2x_i + x_{i+1}) + \frac{1}{2}[(x_{i-1} - x_i)^2 - (x_i - x_{i+1})^2] + \cdots, \tag{3}$$

where both time and displacement are scaled in $\tau = \sqrt{3/2}\delta_0^{1/4} t$ and $x_i = u_i/(2\delta_0)$. The dot is the derivative with τ.

It is well known that the Toda interaction force between two adjacent mass points in TL has the form

$$F_i^T = e^{y_{i-1} - y_i} - 1, \tag{4}$$

where y_i is the dimensionless displacement of the ith mass from the equilibrium position.[17] Thus the equation of motion of each lattice is given as follows:

$$\ddot{y}_i = (y_{i-1} - 2y_i + y_{i+1}) + \frac{1}{2}[(y_{i-1} - y_i)^2 - (y_i - y_{i+1})^2] + \cdots. \tag{5}$$

Hence, Eqs. (3) and (5) have the same form up to the second order. It is interesting to investigate the difference of the dynamical properties of HSWs in the TL and the GC.

Since the same dynamical equation is used to describe the propagation of SW in GC and TL, we consider the single SW solution of the TL as follows:

$$y_i = \ln \frac{1 + e^{2[\beta t - k(i-1)]}}{1 + e^{2(\beta t - ki)}}, \tag{6}$$

where k is wave number and $\beta = \sinh k$ is frequency.[17]

Using Eq. (6) and the incident SWs for parameters $k = 0.3$ and $\delta_0 = 1$ we obtain the right (left) *traveling* solitary wave (RSW/LSW). At the beginning, the center of RSW is placed at grain 100 of the PGC. For the study of the HSWs we initiate two identical perturbations described by Eq. (6) with the same parameters simultaneously at grain 100 and grain 300, respectively. Dynamical simulation is then carried out by solving Eq. (2) to obtain the time evolution of the RSW (blue line) and observe the HSW process (red line) in Fig. 1. Both maximum force and corresponding arrival time of right and left scattered SW (RSSW/LSSW) are observed to be completely symmetrical about grain 200. Thus we just compare the results of the RSW and RSSW when the maximum forces between two adjacent grains reach grains 150, 193, 200, 207, 250, and 300 in Fig. 1.

In Fig. 1, the attenuation of the RSW's amplitude in simulations is clearly visible, which means that some form of scattering happens to the RSW due to the discrete nature of grains in the GC.[23,24] The maximum force at grain 200 is 0.2749 obtained by direct numerical simulation whereas it is 0.2775 when obtained by using the solution of the TL as the initial condition. The data also shows that due to the SW-SW collision, some oscillatory waves with very weak amplitudes form and trail the leading backscattered SW.[20]

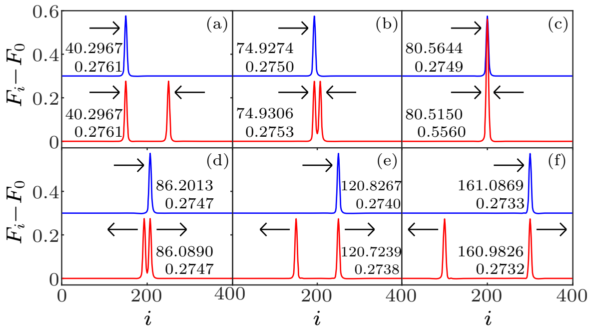

Fig. 1. Dynamics of the RSW (blue line) and the HSW collision process of the two SWs (red line) for the parameters of $k = 0.3$ and $\delta_0 = 1$. Here (a)–(f) show the snapshots when the maximum force on grains 150, 193, 200, 207, 250, and 300 and the instants when the recorded force is achieved are recorded. The data for the RSW is shifted up by 0.3. The arrow stands for the propagation direction of the SWs.

Let us now compare the propagation behavior of the RSW and the RSSW of the HSWs in Fig. 1. This exercise will help understand the process of SW collision in this PGC. We note at the very outset that the chosen initial condition does not lead to a stable SW here but rather mimics a scenario reminiscent of what has been reported in Ref. [20]. This SW solution is quite distinct hence from the SW solution for the uncompressed GC[25] and very slowly loses its energy. The lost energy from the SW ends up in the oscillatory tail of the wave which is too weak to be visible in Fig. 1. Our aim is to see whether any phase shift occurs during the collision of HSWs in the GC. In Fig. 1(a), both maximum force (0.2761) and arrival time (40.2967) of the RSW and the right propagating piece of the HSWs are equal, which means that the HSWs are propagating independently in this stage.

The RSW is at grain 193 and the two HSWs at grains 193 and 207 are shown in Fig. 1(b). The RSW registers a maximum force of 0.2750, which is less than the right propagating piece of the HSWs that yields a maximum force of 0.2753. This increase in the value of the recorded force of the right piece of the HSWs implies the presence of interaction between the right and the left waves that make up the HSWs. Such interaction is expected given that the SWs that make up the HSWs are not distinct in this stage. It is interesting to note that the collision causes a slowdown of the HSWs and results in a larger arrival time, 74.9306 for the right wave of the HSWs which is at 74.9274.

We next observe that the arrival time of two pieces of the HSWs is 80.5150 whereas that of RSW is 80.5644 as shown in Fig. 1(c). In addition, the combined SWs that form from the HSW collision is nonlinear, which is unexpected. The maximum force is 0.5560 which exceeds twice the value registered by the RSW which is 0.2749 and is closer to twice the force registered by the SWs at the very outset in Fig. 1(a).

Once the HSWs get past each other, the arrival time of the right propagating piece of the HSWs is seen to be smaller than that of RSW as shown in Figs. 1(d), 1(e) and 1(f). The arrival times of the right propagating HSWs for grains 207, 220 and 300 are 86.0890, 120.7239, 160.9826, respectively; whereas the corresponding arrival times for the RSW are 86.2013, 120.8267, 161.0869, respectively. This means that, post-collision, the HSWs end up with a phase-lead, which is also an unexpected result.

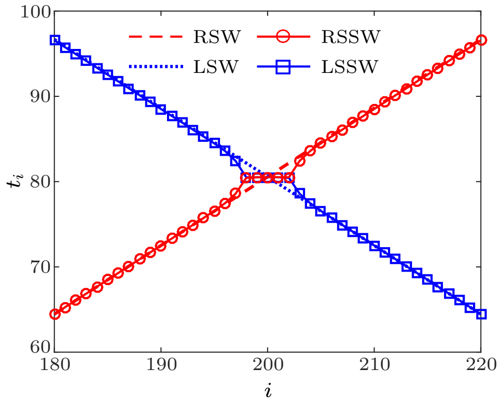

Fig. 2. The arrival time as a function of grain number. The red dashed and blue dotted lines are for RSW and LSW, respectively. The red circles and blue squares are for RSSW and LSSW. The solid lines are a guide for the eyes.

To further explore the phase-lead as a consequence of the collision of HSWs we focus on Fig. 2, which shows the simulation results with arrival times as a function of grain number for RSW, the LSW, and the HSWs. First, complete symmetry of right and left traveling waves is evident from Fig. 2. In Fig. 2, a central collision region of about a five-grain width is identifiable in the vicinity of grain 200, in which the right and left pieces of the HSWs pass through each other in a short time. Further, four kinds of traveling stages can be identified on the sides of the central collision region as follows: (I) pre-in-phase traveling stage—when the left and right moving pieces of the HSWs are still far from each other and do not have any interaction and are traveling independently. The arrival time of the two moving pieces of the HSWs are identical to that of RSW and the LSW. (II) Lag-phase collision state—once the right and left pieces of the HSWs start to interact, nonlinear superposition effect leads to a later arrival time compared to that of the RSW and the LSW, respectively. This effect becomes clearly visible when the right and left components of the HSWs approach the central collision region. Lag-phase collision stage is applicable for the early phase of the collision process. (III) Lead-phase collision state—when the centers of right and left pieces of the HSWs get across each other, we can see that the arrival times of the two waves are always smaller than that of RSW and LSW. Simulation data show that this phase lead effect emerges during the later half of the collision of the HSWs. (IV) Post-in-phase traveling stage—When the LSSW and the RSSW separate significantly away from each other, they lose the mutual interaction and propagate independently again. The waves then get into the post-in-phase stage. In this stage we find that the arrival times of the LSSW and the RSSW are always smaller than that of RSW and the LSW, thanks to the lead-phase collision state.

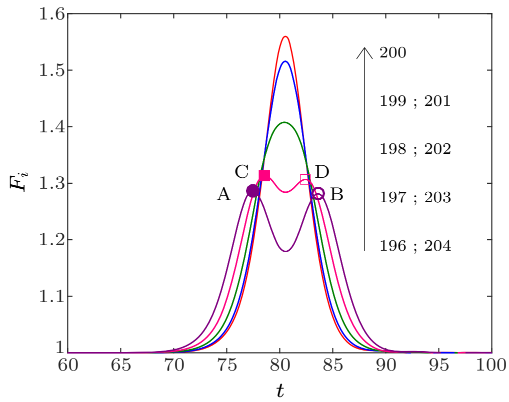

Fig. 3. The interaction force as a function of time for the RSSW and the LSSW.

The simulation results have shown that phase lag and phase lead occur in earlier and later halves of the collision stages, respectively. Furthermore, two kinds of phase shifts cannot be canceled out and general phase lead occurs after the collision. It is interesting to get further insight on the collision characteristic of HSWs around the center of the collision region. The interaction between two adjacent grains around grain 200 as a function of time is plotted in Fig. 3. The interaction forces of symmetrical grains in the collision region (i.e., grains 200, 199, 201, 198, 202) are found to completely coincide at all times. The grains have only one peak, which corresponds to the maximum force at the arrival time. The position of the peak is shifted upward as the grain approaches to grain 200. This single peak formation means that the right and left traveling waves of the HSWs superpose and they can no longer be distinguished during this time of collision. For example, the superposed wave has only one peak as the interaction force between grain 200 and grain 201 gets to the maximum as shown in Fig. 1(c). The two peaks are again seen for grains outside the central collision region such as for grains 197 and 203 and 196 and 204 as shown in Figs. 1(a), 1(b), 1(d), 1(e), and 1(f). Obviously, the peak at an earlier time is larger than that at the later time, $F_{\rm A} > F_{\rm B}$ and $F_{\rm C} > F_{\rm D}$. This attenuation feature arises from the discrete nature of grain compared to the case of TL as alluded to earlier.

Figure 4 shows the left and right propagating pieces of the HSWs moving towards each other. Careful examination of Fig. 4 with the maximum force recorded in grains seen on a log scale reveals the formation of oscillatory waves associated with small scale grain vibrations immediately after the collision. While these oscillations are known to arise in PGCs,[26] it is worth noting how feeble these oscillations are even at the precompressions used in this work and this observation is the most important aspect of the present study. It is this feature of the present work which helps explain the long-lived SWs seen in Ref. [20]. These waves are weak enough to be undetectable when viewed in a linear scale. It is conceivable that the presence of these tail oscillations play a role in the slight speeding up of the LSSW and the RSSW compared to the LSW and the RSW.

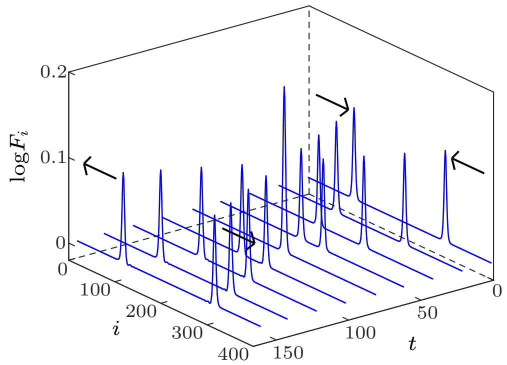

Fig. 4. Here we plot the log of the maximum force as functions of time and grain number. The process of collision of the right and left pieces of the HSWs is shown. Negative values have been removed for the calculation of $\log F_i$ by adding a constant to the actual value of all the force data.

In summary, we have examined the head-on collision of two identical SWs in a precompressed granular chain in this study. Our system is initiated by using the solution to the Toda lattice problem and allowed to evolve via discrete element simulations. We find that the SWs slow down when they approach each other and speed up as they travel past each other. Sufficiently far from the collision region the speed-up and slow-down effects become undetectable. Our studies show that some small oscillations emerge immediately after the SWs collide at the trailing ends of the waves. Overall, the energy carried by these oscillations is orders of magnitude smaller (see Fig. 4) and hence the SWs are expected to live for very, very long times. Such a result is consistent with the results in Ref. [20]. It would be interesting to see if our findings and those of Ref. [20] can be reproduced experimentally. If so, it would confirm the existence of an essentially non-ergodic system across a precompression range for granular chains and would be of wide interest in statistical physics, nonlinear dynamics and engineering.

The authors would like to thank Yannan Shen for providing the numerical source code.

References

[1] Zabusky N J and Kruskal M D 1965 *Phys. Rev. Lett.* **15** 240
[2] Schwarz U T, English L Q and Sievers A J 1999 *Phys. Rev. Lett.* **83** 223
[3] Xie A H, van der Meer L , Hoff W and Austin R H 2000 *Phys. Rev. Lett.* **84** 5435
[4] Fleischer J W, Segev M, Efremidis N K and Christoulids D N 2003 *Nature* **422** 147
[5] Nesterenko V F 1983 *J. Appl. Mech. Tech. Phys.* **24** 733
[6] Coste C, Falcon E and Fauve S 1997 *Phys. Rev. E* **56** 6104
[7] Sokolow A, Bittle E and Sen S 2007 *Europhys. Lett.* **77** 24002
[8] Sun D and Sen S 2013 *Granul. Matter* **15** 157
[9] Sen S, Manciu M and Manciu F S 1999 *Appl. Phys. Lett.* **75** 1479
[10] Vergara L 2005 *Phys. Rev. Lett.* **95** 108002
[11] Liu X Y, Jiao T F, Ma L, Su J Y, Chen W Z, Sun Q C and Huang D C 2017 *Granul. Matter* **19** 55
[12] Breindel A, Sun D and Sen S 2011 *Appl. Phys. Lett.* **99** 063510
[13] Ma L, Huang D C, Chen W Z, Jiao T F, Sun M, Hu F L and Su Y J 2017 *Phys. Lett. A* **381** 542
[14] Hertz H 1881 *J. Reine U. Angew. Math.* **92** 156
[15] Sun D K, Daraio C and Sen S 2011 *Phys. Rev. E* **83** 066605
[16] Herbold E B and Nesterenko V F 2007 *Appl. Phys. Lett.* **90** 261902
[17] Toda M 1998 *Theory of Nonlinear Lattices* (New York: Springer-Verlag)
[18] Wang F G, Yang Y Y, Han J F and Duan W S 2018 *Chin. Phys. B* **27** 044501
[19] Shen Y, Kevrekidis P G, Sen S and Hoffman A 2014 *Phys. Rev. E* **90** 022905
[20] Takato Y and Sen S 2012 *Europhys. Lett.* **100** 24003
[21] Kuwabara G and Kono K 1987 *Jpn. J. Appl. Phys.* **26** 1230
[22] Schăfer J, Dippel S and Wolf D E 1996 *J. Phys. I* **6** 5
[23] Ávalos E and Sen S 2009 *Phys. Rev. E* **79** 046607
[24] Ávalos E, Sun D K, Doney D L and Sen S 2011 *Phys. Rev. E* **84** 046610
[25] Sen S and Manciu M 2001 *Phys. Rev. E* **64** 056605
[26] Manciu M, Tehan V and Sen S 2000 *Chaos* **10** 658